

Proceeding Paper

# Immobilization of Rare Earth Elements and Yttrium (REY) by Iron (Bio)Precipitation in Acid Sulfate Waters from El Bierzo (Spain)<sup>†</sup>

Blanca Rincón-Tomás , Francisco Javier González , Enrique López-Pamo and Esther Santofimia 

Geological Survey of Spain, Spanish National Research Council (IGME-CSIC), 28003 Madrid, Spain; fj.gonzalez@igme.es (F.J.G.); e.lopez@igme.es (E.L.-P.); e.santofimia@igme.es (E.S.)

\* Correspondence: b.rincon@igme.es; Tel.: +34-91-728-7203

<sup>†</sup> Presented at the 2nd International Conference on Raw Materials and Circular Economy “RawMat2023”, Athens, Greece, 28 August–02 September 2023.

**Abstract:** Acid sulfate waters originated from acid rock drainage (ARD), affecting the La Silva stream (El Bierzo, Spain), present anomalously high values of rare earth elements and yttrium (REY). These REY are maintained dissolved along the water stream as sulfate ions forming complexes like  $\text{REYSO}_4^+$  and  $\text{REY}(\text{SO}_4)^{2-}$ . Negatively charged REY complexes seem to have an affinity for iron precipitates found along the La Silva stream and its tributaries since their surface is positively charged at this low pH. The presence of iron-oxidizing bacteria in iron precipitates addresses the possibility of their implication in this REY immobilization and its potential use in (bio)remediation and strategic metal industry applications.

**Keywords:** ARD; iron precipitates; REE; REY; bioprecipitation; *Gallionellaceae*; FeOB



**Citation:** Rincón-Tomás, B.; González, F.J.; López-Pamo, E.; Santofimia, E. Immobilization of Rare Earth Elements and Yttrium (REY) by Iron (Bio)Precipitation in Acid Sulfate Waters from El Bierzo (Spain). *Mater. Proc.* **2023**, *15*, 47. <https://doi.org/10.3390/materproc2023015047>

Academic Editors: Antonios Peppas, Christos Roumpos, Charalampos Vasilatos and Anthimos Xenidis

Published: 16 November 2023



**Copyright:** © 2023 by the authors. Licensee MDPI, Basel, Switzerland. This article is an open access article distributed under the terms and conditions of the Creative Commons Attribution (CC BY) license (<https://creativecommons.org/licenses/by/4.0/>).

## 1. Introduction

Acid rock drainage (ARD) refers to the process of acidic water generation resulting from the exposure and oxidation of sulfides by natural or anthropogenic processes, such as road construction and poorly disposed mine tailings [1]. Black shales contain high concentrations of pyrite, which, upon weathering, produces acid sulfate waters [2]. These waters are characterized by low pH levels and high concentrations of metals and metalloids, including rare earth elements and yttrium (REY) [3,4].

Iron precipitates form in acid sulfate waters enriched in Fe when the pH increases to values > 3, for example, when ARD interacts with natural rivers. The formation of iron precipitates involves the oxidation of ferrous iron ( $\text{Fe}^{2+}$ ) to ferric iron ( $\text{Fe}^{3+}$ ), followed by the hydrolysis of  $\text{Fe}^{3+}$  ions, leading to the precipitation of iron oxyhydroxide and/or oxyhydroxysulfate minerals. Different microbial organisms involved in the formation of iron oxyhydroxides have been reported in sulfated acidic environments [5–7].

Acid sulfate waters from the oxidative dissolution of pyrite in Mid-Ordovician black shales have affected the La Silva stream in El Bierzo, Spain [8]. These black shales were exposed to weathering due to highway construction close to the area. Previous studies have reported an enrichment of thorium (Th), uranium (U), and REY in the water and precipitates of the La Silva stream. The presence of monazite ( $[\text{Ce}, \text{La}, \text{Y}, \text{Th}]\text{PO}_4$ ) and xenotime ( $\text{YPO}_4$ ) seems to be the source of these dissolved elements [2].

This extended abstract comprises a side study of [2] and presents preliminary results of the potential role of iron (bio)precipitates in the retention and accumulation of REY and its industrial applications.

The presence of REY in acid sulfate waters and acid mine drainage environments is of interest due to their economic and technological importance. These elements are crucial

materials for various modern technologies, and their recovery from ARD systems has been investigated [3,9–12].

## 2. Materials and Methods

### 2.1. Sampling Area and Geochemical Analysis

La Silva stream is located east of El Bierzo region in the province of León (NW Spain). It is 7.6 km long and a tributary of the Tremor River. A passive treatment system was constructed along a 2 km stretch of the stream from its source to the town of La Silva. La Silva stream and its tributary Aborregados stream are affected by ARD [8]. Water and precipitate samples are taken along La Silva stream and its tributaries (Figure 1). Water physico-chemical parameters are described in [2].

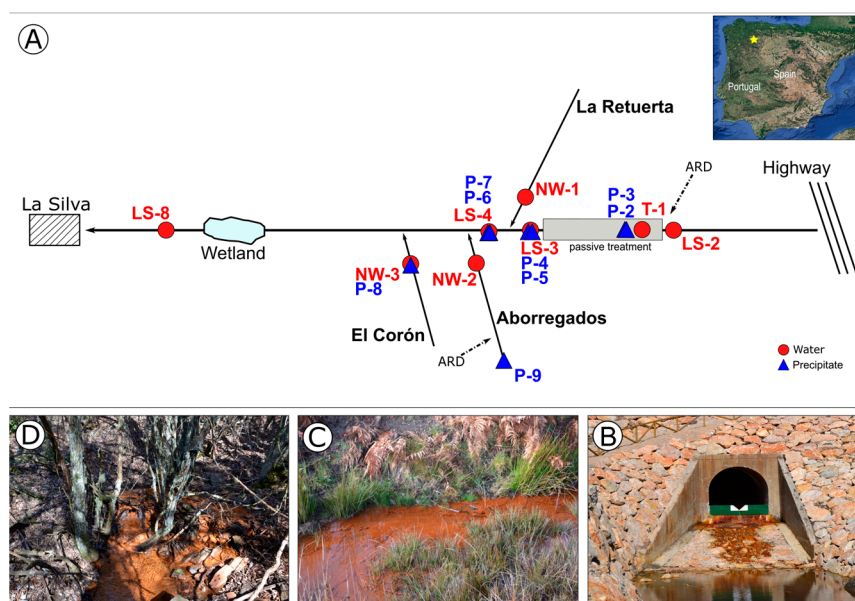


**Figure 1.** Scheme of the sampling area (A) with pictures (B–D) of the most representative sampling sites. Yellow star indicates the geographical location of the sampling area. (B) site where sample LS-3, P-4 and P-5 were taken. (C) site where sample P-9 was taken. (D) site where samples NW-3 and P-8 were taken.

### 2.2. Rare Earth Elements and Yttrium (REY) Measurements

Rare earth elements and yttrium (REY) concentrations were determined in water and precipitates' samples by ICP mass spectrometry (ICP-MS) using an Agilent 7500 ce instrument (Agilent Technologies Inc., Palo Alto, USA) at the Geological Survey of Spain (Madrid, Spain). In the case of the precipitates, samples were previously digested with HF, HClO<sub>4</sub>, and HNO<sub>3</sub> to dryness and dissolution with 7% HNO<sub>3</sub> [2].

### 2.3. Identification and Characterization of Precipitates

X-ray diffraction analysis (XRD), wavelength dispersive X-ray fluorescence (WDXRF), and scanning electron microscopy with EDS (SEM-EDS) analyses were used to accurately identify the mineral phase of the precipitates. SEM-EDS was also used for morphological and 3D textural mineral characteristics on a JEOL JSM-6400 instrument (JEOL, Tokyo, Japan) at the ICTS National Electron Microscopy Center of the Complutense University of Madrid (Madrid, Spain) [2].

### 2.4. Environmental Bacterial 16S Metabarcoding

Microbial partial 16S rRNA gene amplification was performed on DNA extracted from P-8 and P-9 samples. A 300 paired-end Illumina sequencing of the amplicons was carried out in NGS Göttingen, Germany. Resulting sequences were processed using QIIME2-2023.2

and associated plugins [2,9]. R programming was used for data visualization. Raw sequences were deposited in the National Center for Biotechnology Information (NCBI) in the Sequence Read Archive data PRJNA814088. Detailed information and references are found in supplementary data from [2].

### 3. Results and Discussion

#### 3.1. High Concentrations of Rare Earth Elements and Yttrium (REY) in Stream Water

Geochemical measurements revealed a general enrichment of all the samples in REY (Table 1). The oxidation of pyrite promotes acidification of the waters, accelerating the weathering processes and alteration of sulfides and phosphate minerals (xenotime and monazite) that results in the solubilization of LREE (La, Ce, Pr, and Nd) [2]. The highest contents of  $\Sigma$ REY in waters were detected close to the ARD input in the La Silva stream (T-1 and L-3, up to 4086  $\mu\text{g/L}$ ) and the Aborregados stream (NW-2, 2123  $\mu\text{g/L}$ ). In the latter, the enrichment was clearly expressed by the high contents of La, Ce, and Nd (323, 1114, and 302  $\mu\text{g/L}$ , respectively). Interestingly, the La Silva downstream sample (LS-8) presented high  $\Sigma$ REY values (1242  $\mu\text{g/L}$ ), attributed to the absence of aluminum (Al) precipitation at such a low pH since REY have a great affinity to co-precipitate with Al phases [13]. Dissolved REY in these acid sulfate waters forms complexes, mainly  $\text{REY}\text{SO}_4^+$  [14], but also  $\text{REY}(\text{SO}_4)^{2-}$  and the phosphate complex  $\text{Ce}(\text{H}_2\text{PO}_4)^{2+}$  [2].

**Table 1.** Rare earth elements and yttrium (REY) measured in water and precipitate samples ( $\mu\text{g/L}$ ). Extracted and modified from [2].

	Sample	Y	La	Ce	Pr	Nd	Sm	Eu	Gd	Tb	Dy	Ho	Er	Tm	Yb	Lu	REY
Water	LS-2	38.07	44.7	81.16	9.09	34.5	6.89	1.43	8.12	1.21	6.86	1.32	3.51	0.46	3.07	0.49	241
	T-1	749	166	865	86.7	415	113	23.9	143	25.7	158	29.8	79.9	11.4	75.9	11.7	2954
	LS-3	1047	233	1191	119.4	571	157	33.1	197	35	218	40.8	109	15.5	103	16	4086
	LS-4	316	88	399	40.2	187	50.7	10.6	61.5	10.9	67.2	12.6	33.5	4.74	31.5	4.83	1318
	LS-8	181	139	523	41.4	174	39.4	7.7	41.9	6.72	39	7.17	18.7	2.65	17.4	2.76	1242
	NW-1	1.07	15	1.98	0.21	0.99	0.23	0.04	0.23	0.03	0.21	0.04	0.12	0.01	0.12	0.02	20
	NW-2	119	323	1114	77.6	302	57.2	9.87	45.7	5.76	28.4	4.8	12.1	1.61	10.8	1.61	2123
	NW-3	0.32	0.28	0.48	0.07	0.3	0.06	0.01	0.06	0.01	0.04	0.01	0.02	0	0.02	0	2
	Precipitates	P-2	8.81	1.92	14.5	2.43	13.5	4.22	0.85	4.8	0.66	3.53	0.54	1.16	0.15	0.85	0.11
P-3		6.17	2.19	12.8	1.93	11.2	3.47	0.69	3.61	0.5	2.42	0.42	0.89	0.11	0.61	0.08	57
P-4		5.97	1.96	11.2	1.87	10.5	3.28	0.67	3.69	0.5	2.5	0.36	0.8	0.09	0.51	0.07	44
P-5		9.05	2.72	13.6	2.06	12.1	4.39	0.88	5.06	0.69	3.42	0.56	1.23	0.14	0.75	0.09	57
P-6		15.54	7.1	39.3	4.91	25.4	7.13	1.42	6.83	1.06	5.85	1.04	2.6	0.4	2.66	0.4	122
P-7		4.66	0.98	8.97	1.69	9.9	3.17	0.66	3.32	0.43	2.24	0.33	0.76	0.1	0.65	0.08	38
P-9		5.44	10	48.8	2.01	8.13	1.7	0.84	1.6	0.17	1.01	0.21	0.57	0.09	0.63	0.1	81

#### 3.2. Iron (Bio)Precipitates and REY Immobilization

XRD, WDXRF, and SEM-EDS analyses of the precipitates differentiate between three main different types of iron minerals: (i) schwertmannite, which precipitates at  $\text{pH} < 4$  and was detected in P-3, P-4, P-5, and P-7 (Figure 2A); (ii) lepidrocrocite, normally formed at  $\text{pH} > 4.5$  in  $\text{Fe}^{2+}$ -rich environments and low oxygen, found in P-8 and P-9 (Figure 2B); and (iii) goethite, a more stable mineral that sometimes appears as an evolution of the first two iron minerals (P-2, P-5, P-6, and P-9). Iron precipitates presented the highest values of REY under  $\text{pH} 3.5\text{--}4$ , i.e., La Silva downstream (P-6,  $\Sigma$ REY 122  $\mu\text{g/L}$ ) and Aborregados tributary (P-9,  $\Sigma$ REY 81  $\mu\text{g/L}$ ; Table 1). Schwertmannite and goethite are rich in sulfate, with a characteristic Fe/Smolar ratio between 5.2 and 6.4 for schwertmannite, and goethite forms a more stabilized form for schwertmannite [2]. Thus, they presented a great specific surface, probably positively charged due to acidic conditions that promoted the adsorption and therefore immobilization of negatively charged complexes (e.g.,  $\text{REY}(\text{SO}_4)^{2-}$ ), as observed in sample P-6 enriched in LREE and yttrium. Similarly, lepidrocrocite and goethite from

sample P-9 are specifically enriched in La and Ce, probably by the presence of several factors, like phosphate and organic anions acting as ligands.

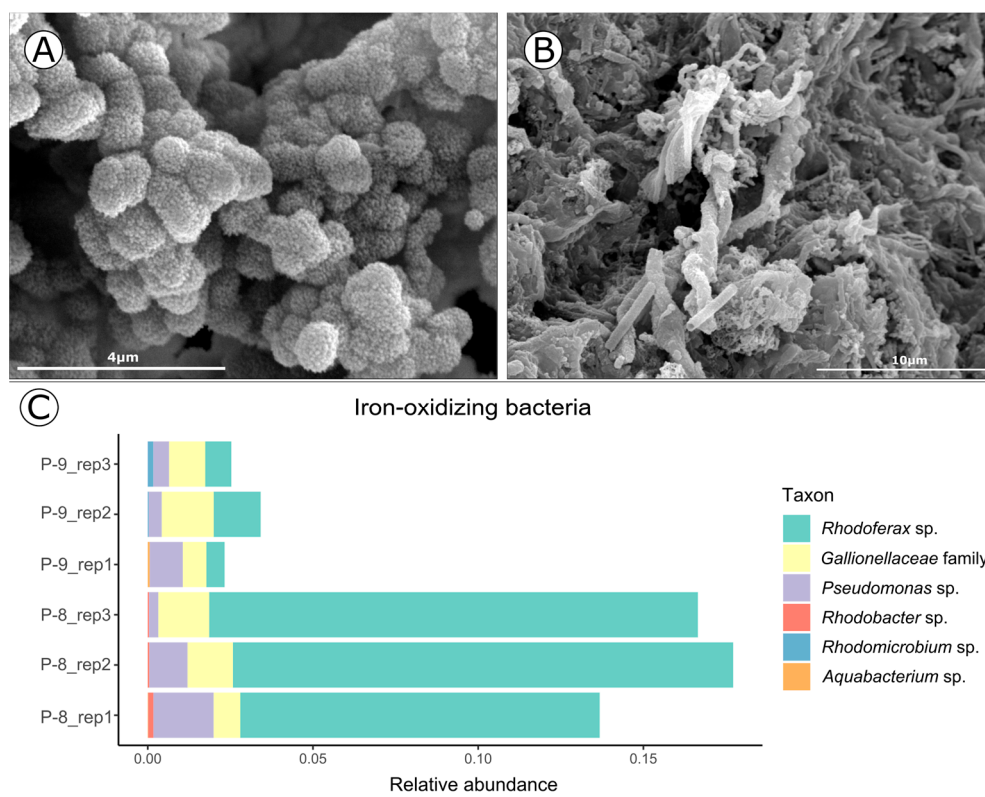


**Figure 2.** SEM micrographs of (A) schwertmannite and (B) lepidocrocite with microbial twisted stalks (B). (C) Bacterial organisms described as potential iron-oxidizers found in P-8 and P-9.

Environmental 16S rRNA gene analyses from lepidocrocite samples revealed the presence of microorganisms involved in the oxidation and precipitation of iron (FeOB), in accordance with the observed twisted stalks (Figure 2B,C). These organisms are mainly from the microaerophilic *Gallionellaceae* family [15] and *Rhodoferrax* sp. [16], pointing out the potential role of microorganisms in the immobilization and therefore accumulation of REY in acid sulfate waters [7].

#### 4. Conclusions

The findings from this study suggest a potential association between the sampled iron precipitates and the precipitation of REY. The enrichment of dissolved REY in acid waters results from the weathering of black shales, which contain dispersal minerals such as monazite and xenotime. The dissolution rate of rocks and the release of solutes into the water are significantly more pronounced and efficient in acidic solutions than in basic solutions. The mixing of ARD with natural waters increases the pH enough to favor iron precipitation like schwertmannite, goethite, and lepidocrocite. These iron precipitates immobilize the REY present in the water streams due to their specific surface area and capacity to uptake REY complexed with sulfates, phosphates, and/or organic compounds that act as ligands.

The presence of iron-oxidizing bacteria and biogenic iron precipitates provides evidence for the possibility of their indirect participation in REY precipitation processes. However, further research is needed to fully understand the extent and mechanisms of microbial participation and involvement in REY precipitation.

**Author Contributions:** Conceptualization, B.R.-T. and E.S.; methodology, B.R.-T. and E.S.; software, B.R.-T. and E.S.; validation, B.R.-T., E.S., F.J.G., and E.L.-P. All authors have read and agreed to the published version of the manuscript.

**Funding:** This work was supported financially with funds from (1) the Spanish Geological Survey (IGME-CSIC) project 2572 “Estudio del origen, migración y puesta en disolución de Torio-Uranio en aguas ácidas”, and (2) the Next-Generation EU MINECRITICAL project (C17.I7, MET2021-00-000).

**Institutional Review Board Statement:** Not applicable.

**Informed Consent Statement:** Not applicable.

**Data Availability Statement:** Detailed data of some of the results used here can be found in the publication of Santofimia et al., 2022 [2], published in *Chemosphere Journal* with DOI:10.1016/j.chemosphere.2022.135907. Raw 16S amplicon sequences can be found in NCBI, in the SRA PR-JNA814088.

**Acknowledgments:** We acknowledge the G2L Next-Generation Sequencing Center of Göttingen and colleagues from geochemical laboratories from the Geological Survey of Spain (IGME-CSIC). This study is a contribution to the Horizon Europe project GSEU (HORIZON-CL5-2021-D3-02-14, Project 101075609).

**Conflicts of Interest:** The authors declare no conflict of interest.

## References

1. Ferguson, K.D.; Morin, K.A. The Prediction of Acid Rock Drainage—Lessons from the Database. In Proceedings of the Second International Conference on the Abatement of Acidic Drainage, Montreal, QC, Canada, 16–18 September 1991.
2. Santofimia, E.; González, F.J.; Rincón-Tomás, B.; López-Pamo, E.; Marino, E.; Reyes, J.; Bellido, E. The mobility of thorium, uranium and rare earth elements from Mid Ordovician black shales to acid waters and its removal by goethite and schwertmannite. *Chemosphere* **2022**, *307*, 135907. [CrossRef] [PubMed]
3. Ayora, C.; Macías, F.; Torres, E.; Lozano, A.; Carrero, S.; Nieto, J.M.; Pérez-López, R.; Fernández-Martínez, A.; Castillo-Michel, H. Recovery of rare earth elements and yttrium from passive-remediation systems of acid mine drainage. *Environ. Sci. Technol.* **2016**, *50*, 8255–8262. [CrossRef] [PubMed]
4. Mastalerz, M.; Drobniak, A.; Eble, C.; Ames, P.; McLaughlin, P. Rare earth elements and yttrium in Pennsylvanian coals and shales in the eastern part of the Illinois Basin. *Int. J. Coal Geol.* **2020**, *231*, 103620. [CrossRef]
5. Ferris, F.G.; Tazaki, K.; Fyfe, W.S. Iron oxides in acid mine drainage environments and their association with bacteria. *Chem. Geol.* **1989**, *74*, 321–330. [CrossRef]
6. Kim, J.; Kim, S.; Tazaki, K. Mineralogical characterization of microbial ferrihydrite and schwertmannite, and non-biogenic Al-sulfate precipitates from acid mine drainage in the Donghae mine area, Korea. *Env. Geol.* **2002**, *42*, 19–31. [CrossRef]
7. Kawano, M.; Tomita, K. Geochemical modeling of bacterially induced mineralization of schwertmannite and jarosite in sulfuric acid spring water. *Am. Mineral.* **2001**, *86*, 1156–1165. [CrossRef]
8. Santofimia, E.; López-Pamo, E. Performance of an open limestone channel for treating a stream affected by acid rock drainage (León, Spain). *Environ. Sci. Pollut. Res.* **2016**, *23*, 14502–14517. [CrossRef]
9. Bolyen, E.; Rideout, J.R.; Dillon, M.R.; Bokulich, N.A.; Abnet, C.C.; Al-Ghalith, G.A.; Alexander, H.; Alm, E.J.; Arumugam, M.; Asnicar, F.; et al. Reproducible, interactive, scalable and extensible microbiome data science using QIIME 2. *Nat. Biotechnol.* **2019**, *37*, 852–857. [CrossRef] [PubMed]
10. Chakhmouradian, A.R.; Wall, F. Rare Earth Elements: Minerals, Mines, Magnets (and More). *Elements* **2012**, *8*, 333–340. [CrossRef]
11. Charalampides, G.; Vatalis, K.I.; Apostoplos, B.; Ploutarch-Nikolas, B. Rare Earth Elements: Industrial Applications and Economic Dependency of Europe. *Procedia Econ. Financ.* **2015**, *24*, 126–135. [CrossRef]
12. Moss, R.L.; Tzimas, E.; Kara, H.; Willis, P.; Kooroshy, J. *Critical Metals in Strategic Energy Technologies*; European Commission: Luxembourg, 2011. [CrossRef]
13. Verplanck, P.L.; Nordstrom, D.K.; Taylor, H.E. Overview of rare earth element investigations in acidwaters of U. S. Geological Survey abandoned minewatersheds. In *U.S. Geological Survey Toxic Substances Hydrology Program—Proceedings of the Technical Meeting, Charleston, South Carolina, 8–12 March 1999*; Morganwalp, D.W., Buxton, H.T., Eds.; Water-Resources Investigations Report 99-4018A; U.S. Geological Survey: West Trenton, NJ, USA, 1999; Volume 99, pp. 83–92.
14. Zhao, F.; Cong, Z.; Sun, H.; Ren, D. The geochemistry of rare earth elements (REE) in acid mine drainage from the Sitai coal mine, Shanxi Province. *North China Int. J. Coal Geol.* **2007**, *70*, 184–192. [CrossRef]

15. Hallbeck, L.; Pedersen, K. The Family *Gallionellaceae*. In *The Prokaryotes*; Rosenberg, E., DeLong, E.F., Lory, S., Stackebrandt, E., Thompson, F., Eds.; Springer: Berlin/Heidelberg, Germany, 2008.
16. Kato, S.; Ohkuma, M. A single bacterium capable of oxidation and reduction of iron at circumneutral pH. *Microbiol. Spectr.* **2021**, *9*, e0016121. [[CrossRef](#)] [[PubMed](#)]

**Disclaimer/Publisher's Note:** The statements, opinions and data contained in all publications are solely those of the individual author(s) and contributor(s) and not of MDPI and/or the editor(s). MDPI and/or the editor(s) disclaim responsibility for any injury to people or property resulting from any ideas, methods, instructions or products referred to in the content.